Gold Redox Chemistry

DOI: 10.1002/anie.201208443

The Redox Chemistry of Gold with High-Valence Doped Calcium Oxide**

Jenni Andersin, Janne Nevalaita, Karoliina Honkala, and Hannu Häkkinen*

Oxide-supported metal catalysts play a central role in the field of heterogeneous catalysis. Controlling the size and shape of the active metal phase is of the utmost importance, as these properties affect the dispersion of the catalytically active metal particles, which in turn reflects the metal–support interaction. The metal–support interactions govern the number and the nature of catalytically active sites; consequently, much of the current research in the field is concentrated on gaining understanding and control of this interaction. Gold is a good example of a metal that becomes catalytically active only in the nanoscale size regime (<5 nm).[1,2] A large amount of recent experimental and theoretical work has shown that the morphology of various oxide supports can be affected by modification of the oxide by either controlling the thickness of the oxide film grown on a metal surface[3,4] or by doping the bulk oxide with higher-valence transition metals.[5,6] Both of these methods rest upon an increase in oxide basicity through modification of the electronic structure of the oxide. A recent analysis of a large number of density functional theory calculations show that the exothermicity of a Lewis acid adsorption increases with the basicity of the oxide surface.[7] The stronger oxide–adsorbate interaction then manifests in a higher wetting propensity of the ad-metal, thus leading to the formation of flat islands.

The stability of planar Au structures on top of the electronically modified oxides has typically been rationalized by the increased adhesion between the electronegative gold and the surface owing to the negative charge on Au. In computations, the stability of the Au/surface system is frequently measured by the adsorption energy (ΔE_{ads}), which is defined as the energy gain upon placing a gold atom or cluster from vacuum onto the oxide surface. The presence of Au modifies both the electronic and atomic structure of the support, particularly in the region between the adsorbate and the dopant. Therefore, the adsorption energy can be expected to be comprised of several terms besides the interaction between the surface and the gold. For example, the considerable energy gain associated with the adsorption of electronegative NO_2 over metal-supported MgO film was found to arise from increased adhesion at the interface between the oxide and the metal support, which resulted from the electron abstraction from the oxide.[8]

Herein, we employ density functional theory (DFT) with the aim of understanding the thermodynamic factors determining Au adsorption energy on high-valence doped CaO. To rationalize the adsorption energy we employ the concept of acid–base interaction,[7] where a high-valence dopant, for example, Mo, acts as a base (donating charge) and Au as an acid (accepting charge). We note that there can be various reasons for a decrease in, or even the prevention of charge transfer from the dopant to the Au; for example, different defect sites can take over dopant-donated electrons.[9] Electron transfer from the dopant to Au might be also kinetically hindered and the exact mechanism of charge transfer is not known. Unlike what is generally proposed in the literature, we herein show that, the charging of Au does not explain the strong Au adsorption on high-valence doped CaO. Instead, the dominant contributions to ΔE_{ads} arise from the energy gain associated primarily with a redox process, where dopant oxidation and Au reduction take place, and secondarily with the iono-covalent interaction between gold and the topmost oxide layer. Screened Coulomb interaction between the charged Au species and the support plays a negligible role in the case of realistic supports, where several undoped oxide layers are grown as buffer over the doped oxide.[5] Considering a few high-valent transition-metal dopants near Mo in the periodic table, we show that for defect-free doped CaO the redox energy determines ΔE_{ads} and correlates with the third ionization energy of the dopant. Our results demonstrate that understanding the redox chemistry in the support is of paramount importance to achieve better control of the morphology of Au nanostructures on doped oxides.

First, we selected Mo as a model dopant. Figure 1 a shows a typical setting of a calculation, where one Au binds to a Mo-doped CaO(100) slab, but never directly to Mo. In all calculations, we have employed a 10 monolayer-thick CaO slab and varied the Mo position from the 2nd oxide layer down to the 7th layer. One dopant per computational unit cell corresponds to the fixed dopant concentration of 1.25%, denoted as $Ca_{98.75}Mo_{1.25}O$ and referred to hereafter as CaMoO. Calculated energy changes, atom charges, and magnetic moments for Mo are compiled in Table S1 in the Supporting Information, and the energetics as a function of a dopant depth is shown in Figure 1 b.

On pristine CaO, the Au atom binds to an oxygen ion with $\Delta E_{ads} = -1.39$ eV, which is close to the value of -1.35 eV reported by Shao et al.[5] At this site no charging of Au is observed based on the empty Au spin-down 6s-state in the

[*] Dr. J. Andersin, J. Nevalaita, Dr. K. Honkala, Prof. Dr. H. Häkkinen
Departments of Chemistry and Physics, Nanoscience Center, University of Jyväskylä, Box 35, 40014 Jyväskylä (Finland)
E-mail: karoliina.honkala@jyu.fi

[**] This work was supported by the Academy of Finland. Computer resources were provided by the University of Jyväskylä Nanoscience Center and CSC—the Finnish IT Center for Science. We thank Prof. N. Lopez and Dr. L. Lehtovaara for useful discussions.

Supporting information for this article is available on the WWW under http://dx.doi.org/10.1002/anie.201208443.

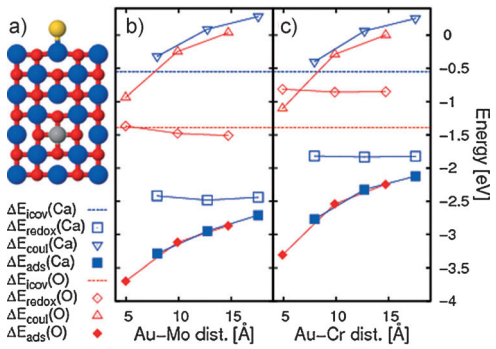

Figure 1. a) Side view of the upper part of the computational unit cell used to model doped CaO with a Au adatom. O red, Ca blue, Au yellow, dopant grey. b, c) Adsorption site-specific energy changes upon iono-covalent bonding of Au on top of pristine CaO (ΔE_{icov}), redox reaction between the Au and dopant (ΔE_{redox}; as a function of dopant depth), and the electrostatic interaction between Au and dopant (ΔE_{coul}; as a function of the Au-dopant distance). The adsorption energy (ΔE_{ads}) is the sum of these three terms. The lines connecting the data points are drawn to guide the eye. The data for Mo and Cr dopants are shown in (b) and (c), respectively.

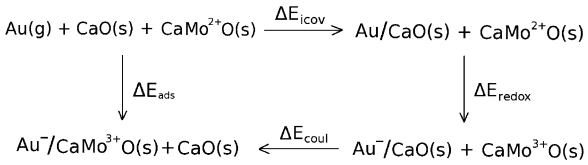

Scheme 1. The Born–Haber cycle for the adsorption of Au onto Mo-doped CaO. The adsorbate–surface interaction (the conventionally calculated adsorption energy, ΔE_{ads}) is divided into three contributions: 1) the iono-covalent bonding of the Au atom onto the pristine CaO surface (ΔE_{icov}), 2) the redox reaction between Au and Mo that leads to charged species still formally at infinite separation (ΔE_{redox}), and 3) the screened electrostatic interaction between the anion and the cation through the dielectric medium (ΔE_{coul}).

PDOS plot (PDOS = atom-projected density of electron states; Supporting Information, Figure S2). Replacement of a Ca cation by Mo leaves four unused electrons, thus turning it into a Lewis base. Upon Au adsorption from the gas-phase, this leads to Au reduction, Mo oxidation, and to a considerably larger ΔE_{ads}, owing to acid-base stabilization. The adsorption energy is doubled on an O site, even if the impurity atom is located well below the surface layer. This long-range effect shows that a direct overlap between the Au and Mo states is not responsible for the observed stabilization. Au bound on top of a Ca cation on pristine CaO yields a relatively low ΔE_{ads} (−0.55 eV), whereas on doped CaO the adsorption is more than 2.5 eV stronger. The results for Au on pristine CaO show that the charging of Au cannot be responsible for the increase in the adsorption energy. Our analysis shows that also on pristine CaO, where ΔE_{ads} is low, Au is anionic: The Au charge (−0.46 | e |) is modest compared to ca. −0.8 | e |, which is the charge gained in the presence of Mo, but the PDOS analysis shows that both of the Au 6s spin-levels become occupied on the Ca-top site (Figure S2). Moreover, the magnetic moment of Au vanishes (Table S1), and the Au–Ca bond distance is very close (3.03 Å vs. 2.97 Å) to the Mo-doped case.

For further analysis, we devised a Born–Haber cycle for the adsorption process of Au onto doped CaO (Scheme 1). In that cycle, the Au–CaMoO interaction is broken down into three contributions. The details on how these contributions are evaluated from DFT calculations are shown in the Supporting Information text. The first one has already been addressed: the direct iono-covalent interaction between the gold and the surface ion involving orbital overlapping, and also the charging of Au on top of Ca. The energy change related to this process is denoted ΔE_{icov}. The Au–Mo interaction is divided into two contributions: 1) the redox process between Au and Mo (ΔE_{redox}), and 2) the electrostatic energy between the Au^- and Mo^{3+} ions formed (ΔE_{coul}). Negative values denote exothermic process. The site-specific energy contributions, as well as their sum (ΔE_{ads}) are plotted as a function of Mo depth in Figure 1b. The different terms vary for the two Au adsorption sites (Ca/O), but sum up to give very similar site-independent adsorption energies.

Next, ΔE_{redox} and ΔE_{coul} terms are discussed in more detail. The initial state of the redox process involves Au adsorption on pristine CaO infinitely far from the Mo-doped part of the surface. The final state is obtained by adding an electron to Au/CaO and removing one from CaMoO. An analysis of the bond lengths, atom charges, and magnetic moments in the charged systems shows that the electron is adopted by Au and donated by Mo. The quantity ΔE_{redox} thus describes the energy gain related to the electron exchange between the Au and Mo. Since the Au already gains charge upon adsorption onto a Ca-site on pristine CaO, the redox energy change involving Au at Ca can be roughly assigned to the system stabilization from Mo oxidation. The more cationic Mo^{3+} exhibits stronger binding to its anionic O^{2-} neighbors, which is manifested by the decreased distances between the Mo^{3+} and its surrounding oxygen atoms. For example, the distance from 3rd layer Mo to the 2nd layer oxygen above is decreased by 6.2% upon positive charging. Because this effect is well localized around the dopant, it should not depend on the Mo depth. Indeed, the ΔE_{redox} value quickly saturates to −2.5 eV when moving towards bulk CaO, as illustrated in Figure 1b. When Au is initially bound to a surface O atom (Au is still neutral), a simultaneous charging of Au and Mo takes place during the redox process. As the redox energy change now saturates to ca. −1.5 eV when Mo moves to the deeper atomic layers, the Au–O interaction must become more repulsive by ca. 1 eV, owing to the Au reduction. The repulsion between the negative species is clearly reflected in the Au–O bond length, which increases from 2.26 to 2.90 Å upon Au reduction.

In the last step of the Born-Haber cycle, the interaction of the charged species is considered in the same computational cell to produce the energy contribution ΔE_{coul}. While the redox energy remains essentially constant as a function of the Mo depth, the ΔE_{coul} demonstrates an approximate $1/r$ behavior, where r is the distance between Au and Mo, as shown in Figure 1b. This confirms that the stabilization energy ΔE_{coul} can be attributed to the electrostatic interaction between the Au anion and Mo cation. However, due to the

strong screening of the Coulomb interaction by the polarized oxide (see Ref. [4c] and Figure S3), this interaction is significant (stronger than −0.5 eV) only at quite short Au–Mo distances where $r < 8$ Å, which corresponds to about 3 CaO layers. In recent experiments, a buffer region of a few undoped CaO layers was grown on top of the doped CaO to isolate gold from the Ca_xMo_yO impurity layers.[5] Therefore, Figure 1b lets us conclude that the screened Coulomb interaction plays virtually no role in the adsorption of gold over this support, but ΔE_{ads} is dominated by the contributions from iono-covalent bonding and the Au–Mo redox process. This conclusion also holds for Au adsorption onto the Cr-doped CaO, as illustrated in Figure 1c, which displays the variation of the adsorption energy as a function of the Cr depth and the contribution from the different energy terms. The comparison of Au adsorption energies shows that the stabilization on Cr-doped CaO is smaller than on Mo-doped CaO. This is mainly due to the difference in redox energy, whereas electrostatic interactions are identical. Bader charges and magnetic moments (Table S2) support the conclusion that Au obtains an electron from Cr, which donates three electrons altogether. The smaller redox energy originates from the higher 3rd ionization energy of Cr compared to Mo, whereas geometric differences are minor (Table S4). These results invoke the question of whether redox energies would generally correlate in the measured 3rd ionization energies of elements. Figure 2 shows that this indeed is true. Thus, with increasing 3rd ionization energy of the dopant, the adsorption energy of a single Au atom decreases.

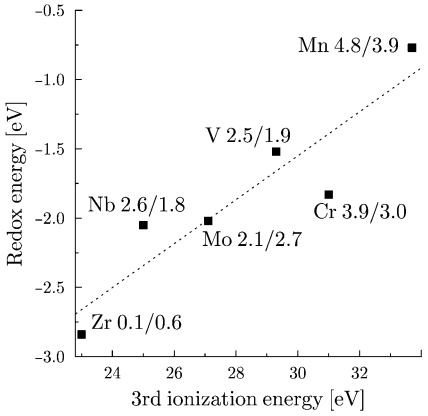

Figure 2. Redox energy plotted as a function of the measured 3rd ionization energy of the different dopants in the CaO(100) slab. The notations μ(2+) and μ(3+), given after the name of the element, refer to the magnetic moments of double and triple cations of the dopants, respectively.[14]

Thus far we have focused on a single Au atom, whereas next we study the adsorption of several separated Au atoms in the same computational unit cell. In agreement with previous results, our calculations show that Mo can oxidize further.[5,9] According to our analysis, Mo can donate up to four electrons to redox reactions, which completely depletes the 4d–5s shells, giving a formal oxidation state of 6+. The higher oxidation of Mo is reflected in the Mo−O bond lengths, which gradually decrease from 2.3 Å for Mo^{2+} to 2.1 Å for Mo^{6+} (CaMoO slab with charge 4+). We estimated the redox energy upon higher oxidation by calculating $\Delta E_{redox}(n)$, where n is the number of electrons donated by one Mo to n non-interacting surface gold atoms (on Ca top sites). The obtained values are −2.44, −2.94, −2.78, and −2.24 eV for $n = 1$–4. This implies that the Mo oxidation state 4+ ($n = 2$) is the most energetically favorable, yielding the maximal $|\Delta E_{redox}(n)|$, after which the electron abstraction no longer increases the Mo–O interaction inside the lattice. Cr behaves differently. The calculated $\Delta E_{redox}(n)$ values are −1.82, −1.42, −0.68, and +0.29 eV for $n = 1$–4. Compared to Mo, these energies are less exothermic, they decrease monotonously, and show that Cr^{3+} is the most favorable oxidation state (Figure S4). The values clearly indicate that Cr is a less efficient multi-valent dopant than Mo: the number of Cr atoms must be higher to transfer the same number of electrons as transferred by Mo.

In conclusion, we have modeled Au adsorption on the high-valence doped calcium oxide surface, rationalized the adsorption with the concept of acid–base interaction, and analyzed the origin of this through the Born–Haber cycle. Redox energy was identified as the main contribution in the adsorption. The leading component of this is the relaxation of dopant–oxide bonds resulting from electron transfer. The stabilization and the removal of the site preference facilitate the formation of the experimentally observed 2D islands.[5] We find a good correlation between redox energy and the 3rd ionization energy of the dopant, which opens the possibility of predicting the effect of the dopant on the adsorption energy of the Au atom. Similar calculations based on the Born–Haber cycle can be employed to analyze adsorption energies of the other adsorbates on various low- and high-valence doped oxide surfaces.

Methods

The DFT calculations were done by using the GPAW implementation[10] of the projector augmented wave (PAW) method[11] in real space grids. The exchange and correlation functional was approximated with the spin-polarized Perdew–Burke–Ernzerhof (PBE) formula.[12] The frozen core and projectors were generated with scalar relativistic corrections for Au. The details of the computational setup for the slab geometry used to model the Mo support, CaO film, dopants, and adsorbates are described in the Supporting Information. Atom charges were analyzed using the Bader method.[13]

Received: October 19, 2012
Published online: December 13, 2012

Keywords: cluster morphology · density functional calculations · gold · nanocatalysis · redox chemistry

[1] a) M. Haruta, *Catal. Today* **1997**, *36*, 153; b) G. C. Bond, D. Thompson, *Catal. Rev. Sci. Eng.* **1999**, *41*, 319; c) M. Valden, X. Lai, D. W. Goodman, *Science* **1998**, *281*, 1647; d) R. Meyer, C. Lemire, S. Shaikhutdinov, H.-J. Freund, *Gold Bull.* **2004**, *37*, 72.

[2] a) A. Sanchez, S. Abbet, U. Heiz, W.-D. Schneider, H. Häkkinen, R. N. Barnett, U. Landman, *J. Phys. Chem. A* **1999**, *103*, 9573; b) H. Häkkinen, S. Abbet, A. Sanchez, U. Heiz, U. Landman, *Angew. Chem.* **2003**, *115*, 1335; *Angew. Chem. Int. Ed.* **2003**, *42*,

1297; c) B. Yoon, H. Häkkinen, U. Landman, A. Wörz, J.-M. Antonietti, S. Abbet, K. Judai, U. Heiz, *Science* **2005**, *307*, 403; d) N. Lopez, T. V. W. Janssens, B. S. Clausen, Y. Xu, M. Mavrikakis, T. Bligaard, J. K. Nørskov, *J. Catal.* **2004**, *223*, 232; e) L. M. Molina, B. Hammer, *Phys. Rev. B* **2004**, *69*, 155424; f) S. Laursen, S. Linic, *Phys. Rev. Lett.* **2006**, *97*, 026101; g) H. Falsig, B. Hvolbæk, I. S. Kristensen, T. Jiang, T. Bligaard, C. H. Christensen, J. K. Nørskov, *Angew. Chem.* **2008**, *120*, 4913; *Angew. Chem. Int. Ed.* **2008**, *47*, 4835; h) O. Lopez-Acevedo, K. A. Kacprzak, J. Akola, H. Häkkinen, *Nat. Chem.* **2010**, *2*, 329.

[3] a) H. M. Benia, X. Lin, H. J. Gao, N. Nilius, H. J. Freund, *J. Phys. Chem. C* **2007**, *111*, 10528; b) M. Sterrer, T. Risse, M. Heyde, H.-P. Rust, H.-J. Freund, *Phys. Rev. Lett.* **2007**, *98*, 206103; c) N. Nilius, *Surf. Sci. Rep.* **2009**, *64*, 595; d) H.-J. Freund, G. Pacchioni, *Chem. Soc. Rev.* **2006**, *35*, 146804.

[4] a) G. Pacchioni, L. Giordano, M. Baistrocchi, *Phys. Rev. Lett.* **2005**, *94*, 226203; b) D. Ricci, A. Bongiorno, G. Pacchioni, U. Landman, *Phys. Rev. Lett.* **2006**, *97*, 036106; c) K. Honkala, H. Häkkinen, *J. Phys. Chem. C* **2007**, *111*, 4319; d) P. Frondelius, H. Häkkinen, K. Honkala, *New J. Phys.* **2007**, *9*, 339; e) P. Frondelius, H. Häkkinen, K. Honkala, *Phys. Rev. B* **2007**, 76, 073406; f) P. Frondelius, A. Hellman, K. Honkala, H. Häkkinen, H. Grönbeck, *Phys. Rev. B* **2008**, *78*, 085426; g) V. Simic-Milosevic, M. Heyde, N. Nilius, T. Konig, H. P. Rust, M. Sterrer, T. Risse, H. J. Freund, L. Giordano, G. Pacchioni, *J. Am. Chem. Soc.* **2008**, *130*, 7814; h) X. Lin, N. Nilius, H.-J. Freund, M. Walter, P. Frondelius, K. Honkala, H. Häkkinen, *Phys. Rev. Lett.* **2009**, *102*, 206801; i) P. Frondelius, H. Häkkinen, K. Honkala, *Phys. Chem. Chem. Phys.* **2010**, *12*, 1483; j) X. Lin, N. Nilius, M. Sterrer, P. Koskinen, H. Häkkinen, H.-J. Freund, *Phys. Rev. B* **2010**, *81*, 153406.

[5] a) X. Shao, S. Prada, L. Giordano, G. Pacchioni, N. Nilius, H.-J. Freund, *Angew. Chem.* **2011**, *123*, 11728 – 11731; *Angew. Chem. Int. Ed.* **2011**, *50*, 11525 – 11527; b) X. Shao, N. Nilius, H.-J. Freund, *Phys. Rev. B* **2012**, *85*, 115444.

[6] N. Mammen, S. Narasimhan, S. de Gironcoli, *J. Am. Chem. Soc.* **2011**, *133*, 2801 – 2803.

[7] H. Metiu, S. Chrétien, Z. Hu, B. Li, X. Sun, *J. Phys. Chem. C* **2012**, *116*, 10439 – 10450.

[8] H. Grönbeck, *J. Phys. Chem. B* **2006**, *110*, 11977 – 11981.

[9] F. Stavale, X. Shao, N. Nilius, H.-J. Freund, S. Prada, L. Giordano, G. Pacchioni, *J. Am. Chem. Soc.* **2012**, *134*, 11380 – 11383.

[10] a) J. J. Mortensen, L. B. Hansen, K. W. Jacobsen, *Phys. Rev. B* **2005**, *71*, 035109; b) J. Enkovaara et al., *J. Phys. Condens. Matter* **2010**, *22*, 253202. The code is available at: https://wiki.fysik.dtu.dk/gpaw.

[11] P. E. Blöchl, *Phys. Rev. B* **1994**, *50*, 17953.

[12] J. P. Perdew, K. Burke, M. Ernzerhof, *Phys. Rev. Lett.* **1996**, *77*, 3865.

[13] a) R. Bader, *Atoms in Molecules*, Oxford University Press, **1990**; b) G. Henkelman, A. Arnaldsson, H. Jonsson, *Comput. Mater. Sci.* **2006**, *36*, 354.

[14] Values for the 3rd ionization energy are taken from http://www.webelements.com.

